Membrane Interactions and Conformational Preferences of Human and Avian Prion N-Terminal Tandem Repeats: The Role of Copper(II) Ions, pH, and Membrane Mimicking Environments

Giuseppe Di Natale,[†] Giuseppe Pappalardo,[‡] Danilo Milardi,[‡] Michele F. M. Sciacca,[†] Francesco Attanasio,[‡] Diego La Mendola,[‡] and Enrico Rizzarelli*[,†]

Dipartimento di Scienze Chimiche, Università degli Studi di Catania, Viale Andrea Doria 6, 95125 Catania, Italy, and Istituto di Biostrutture e Bioimmagini - Catania, Consiglio Nazionale delle Ricerche, Viale Andrea Doria 6, 95125 Catania, Italy

Received: April 13, 2010; Revised Manuscript Received: August 11, 2010

The flexible N-terminal domain of the prion protein (PrP^c) is believed to play a pivotal role in both trafficking of the protein through the cell membrane and its pathogenic conversion into the β sheet-rich scrapie isoform (PrP^{sc}). Unlike mammalian PrP^c, avian prion proteins are not known to undergo any pathogenic conformational conversions. Consequently, some critical advances in our understanding of the molecular mechanisms underlying prion pathogenesis are expected from comparative studies of the biophysical properties of the N-terminal domains of the two proteins. The present study addresses the role played by different environmental factors, i.e., copper(II), pH, and membrane-mimicking environments, in assisting the conformational preferences of huPrP60-91 and chPrP53-76, two soluble peptides encompassing the N-terminal copper(II) binding domains of the human and chicken prion proteins, respectively. Moreover, the membrane interactions of huPrP60-91, chPrP53-76, and their copper(II) complexes were evaluated by Trp fluorescence in conjunction with measurements of the variation in thermotropic properties of 1,2-dipalmitoyl-sn-glycero-3-phosphocholine (DPPC) unilamellar vesicles. Circular dichroism experiments revealed that huPrP60-91 adopts a predominant polyproline II conformation in aqueous solution that is destabilized at basic pH or in the presence of trifluoroethanol (TFE). Unlike anionic sodium dodecyl sulfate (SDS), which seems to stabilize the polyproline II conformation further, zwitterionic dodecylphosphocholine (DPC) micelles do not affect the peptide structure. On the contrary, copper(II) promptly promotes an increase in β-turn-rich structures. Differential scanning calorimetry (DSC) and Trp fluorescence assays carried out on DPPC model membranes after incubation with huPrP60-91 showed a marked tendency of the peptide to slowly penetrate the lipid bilayer with a concomitant conformational transition toward an extended β-sheet-like structure. Such an event, which was ascribed to the hyrophobic Trp side chain residues, was shown to also depend on the level of copper(II) occupancy along the peptide. Conversely, the CD spectra of chPrP53-76 aqueous solutions indicated the presence of a mixture of random-coil/β-turn-like structures whose resulting equilibrium was influenced by SDS and copper(II) addition. Furthermore, chPrP53-76 did not exhibit any tendency to interact with model membranes in either the presence or absence of copper(II). The results reported here provide evidence of the different roles played by environmental factors in affecting the conformation and membrane activity of human and avian prion N-terminal domains.

Introduction

Prion diseases are associated with the accumulation of a misfolded pathogenic form (PrP^{sc}) of the endogenous prion protein (PrP^c), a membrane-bound glycoprotein normally expressed in the central nervous system (CNS) of all mammals.[1–3] Nuclear magnetic resonance (NMR) studies performed on recombinant human PrP^c proteins demonstrated that the C-terminal region, starting approximately at residue 125, adopts a globular fold that is largely helical, along with a small two-stranded β-sheet. Conversely, the N-terminal region, containing approximately 120 residues, is unstructured and flexible in solution.[4–6] There are currently no high-resolution structures for PrP^{sc}, but it is known that the β-sheet content is increased during pathogenic conversion.[7,8] The globular fold of the mammalian PrP^c is also maintained in the avian counterpart[9,10] and both N-terminal domains are featured by tandem amino-acid repeats (PHNPGY in avians, PHGGGWGQ in mammals).[11–13] Notably, prion diseases are only observed in mammals, appearing to be precluded from occurring in avian species.[14]

The physiological function of PrP^c is unknown, even if it is widely recognized that the prion protein binds copper in vivo, and this interaction is required for its biological role.[15–18] In particular, copper is required for PrP^c endocytosis from the extracellular space to the cell interior.[19,20] The different environmental factors, i.e., copper(II), pH, and lipid/water interfaces, experienced by PrP^c during its normal cell cycle may affect the conformational integrity of the protein and, consequently, they are believed to play a critical role in prion pathogenesis.[21]

Several lines of evidence support the hypothesis that the N-terminal domain of prion proteins plays a central role in all these processes: in particular, a number of studies with several

* To whom correspondence should be addressed. Phone: (++39) (0) 95 7385070. Fax: (++39) (0) 95 337678. E-mail: erizzarelli@unict.it.
[†] Università degli Studi di Catania.
[‡] Consiglio Nazionale delle Ricerche.

10.1021/jp1033036
Published on Web 10/11/2010

human prion protein fragments indicate that the main lipid-binding region in the full-length huPrP is located within the N-terminal segment.[22–25] It is also known that the N-terminal domain of huPrP can bind up to six Cu^{2+} ions passing through a series of different binding modes as a function of the metal/peptide ratio.[26,27] The analogous N-terminal domain of the avian prion protein shows differences in the copper(II) binding mode when compared with the human segment.[28] In fact, it has been reported that the tetrahexapeptide Ac-$(PHNPGY)_4$-NH_2 can bind no more than two Cu^{2+} ions[29] and that the predominant complex species is a macrochelate in which the metal ion is coordinated by imidazole nitrogen atoms of the four His residues.[29–32] These differences are likely to exert distinct effects on the structural rearrangements of human and avian N-terminal domains in the presence or absence of Cu^{2+} and membranes.

As a matter of fact, despite the widely recognized roles played by copper(II) and membranes in both the physiological functions and pathogenic conversion of PrP^c, there are no systematic studies assessing the role of Cu^{2+} binding in driving the membrane interactions of prion N-terminal domains. In this light, a comparative study of the biophysical behavior of avian and mammalian N-terminal domains is expected to provide clues about the early steps initiating prion pathogenesis.

In the present work we assessed the conformational properties and membrane interactions of both human Ac-$(PHGGGWQ)_4$-NH_2 (huPrP60-91) and chicken Ac-$(PHNPGY)_4$-NH_2 (chPrP53-76) prion protein N-terminal repeats in the presence of copper(II) ions. Circular dichroism (CD) experiments were carried out to study the conformational preferences of huPrP60-91 in different experimental conditions i.e., pH, solvents, copper(II), and several membrane-like environments. Previously reported data assessing the conformational behavior of chPrP53-76[33] were complemented by further CD experiments in the present study, which were carried out in several membrane-like environments and compared with the results obtained for huPrP60-91. Differential scanning calorimetry (DSC) experiments were performed to evaluate the ability of huPrP60-91, chPrP53-76, and their copper(II) complexes to interact with 1,2-dipalmitoyl-*sn*-glycero-3-phosphocholine (DPPC) model membranes. Finally, Trp fluorescence measurements were carried out on huPrP60-91 to assess the role played by Trp side chains in driving peptide insertion into the lipid matrix.

Materials and Methods

Chemicals. All N-fluorenylmethoxycarbonyl (Fmoc)-protected amino acids and the TGR resin were obtained from Novabiochem; 2-(1*H*-benzotriazol-1-yl)-1,1,3,3-tetramethyluronium tetrafluoroborate (TBTU) and *N*-hydroxybenzotriazole (HOBT) were purchased from Inbios (Naples, Italy); *N*,*N*-diisopropylethylamine (DIEA), triisopropylsilane (TIS), 1,2-dipalmitoyl-*sn*-glycero-3-phosphocholine (DPPC), trifluoroacetic acid (TFA), ethanedithiol (EDT), and trifluoroethanol (TFE) were purchased from Fluka (St. Louis, MO, U.S.); *N*,*N*-dimethylformamide (DMF) was obtained from Lab-Scan (Gliwice, Poland); $Cu(SO_4)_2 \cdot 5H_2O$, $Na_2HPO_4 \cdot 7H_2O$, $NaH_2PO_4 \cdot H_2O$, sodium dodecyl sulfate (SDS), piperidine, and *N*-ethylmorpholine (NEM) were purchased from SIGMA/Aldrich (St. Louis, MO, U.S.). Wholly synthetic dodecylphosphocholine (DPC) was purchased from Avant Polar Lipids (Alabaster, AL, U.S.). All chemicals were of the highest available grade and were used without further purification.

Peptide Synthesis. The peptides Ac-$(PHGGGWGQ)_4$-NH_2 (huPrP60-91) and Ac-$(PHNPGY)_4$-NH_2 (chPrP53-76) were synthesized with the N- and C-termini blocked on a Pioneer peptide synthesizer using the same protocols and instrumental conditions previously reported.[29,34] Preparative reversed-phase high-performance liquid chromatography (rp-HPLC) was carried out on a Varian PrepStar 200 model SD-1 chromatography system equipped with a Prostar photodiode array detector with detection at 222 nm. Purification was performed by eluting with solvents A (0.1% TFA in water) and B (0.1% TFA in acetonitrile) on a Vydac C_{18} 250 × 22 mm (300 Å pore size, 10−15 μm particle size) column, at a flow rate of 10 mL/min. The peptides were eluted using the following chromatographic conditions. (i) huPrP60-91: from 0 to 8 min isocratic gradient in 20% B, then linear gradient from 20% to 30% B over 16 min, finally, isocratic gradient in 30% B from 16 to 25 min; yield = 60% (R_t = 21.30 min). (ii) chPrP53-76: from 0 to 8 min isocratic gradient in 5% B, then linear gradient from 5% to 25% B over 20 min, finally, isocratic gradient in 25% B from 20 to 30 min; yield = 70% (R_t = 25.30 min). The elution profiles were monitored at 222 and 278 nm, and the peptide fractions were collected and lyophilized. Peptide purity was checked by analytical rp-HPLC using a Waters 1525 instrument equipped with a Waters 2996 photodiode array detector with detection at 222 nm on a Vydac C_{18} chromatographic column 250 × 4.6 mm (300 Å pore size, 5 μm particle size), run at a flow rate of 1 mL/min. Sample identity and integrity even after prolonged incubation in aqueous solutions were routinely confirmed by ESI-MS. Calculated mass for huPrP60-91, $C_{142}H_{181}N_{49}O_{37}$: 3164.38. Observed, *m*/*z*: $[M + 2H]^{2+}$, 1583.7; $[M + 3H]^{3+}$, 1056.5; $[M + 4H]^{4+}$, 792.7. Calculated mass for chPrP53-76, $C_{126}H_{161}N_{37}O_{29}$: 2656.23. Observed, *m*/*z*: $[M + 2H]^{2+}$, 1329.11; $[M + 3H]^{3+}$, 886.41; $[M + 4H]^{4+}$, 665.06.

Peptide Preparation in DPC and SDS Micelles. The DPC micelles were prepared as described elsewhere.[35] Briefly, DPC was first dissolved in chloroform and dried in a round-bottomed flask until a thin film of DPC was formed inside. Milli-Q water, preadjusted to pH 7.0, was added to the DPC. The solution was then ultrasonicated in an ultrasonication bath until all of the DPC was dissolved. The SDS was directly dissolved in distilled, deionized water at pH 7.0 to obtain a stock solution. The peptides were dissolved separately in Milli-Q water at pH 7.0. Aliquots of DPC or SDS stock solutions were separately added to a proper amount of peptide stock solutions to obtain samples at different concentrations of surfactant. Considering the critical micellar concentrations (cmc_{DPC} = 1 mM; cmc_{SDS} = 1−10 mM), only samples with DPC and SDS concentration equal to or higher than the cmc value contained micellar aggregates. Finally, each sample was ultrasonicated for 3−5 min, with a 1 min break between each sonication.

Preparation of DPPC Model Membranes. The DPPC model membranes were prepared as described elsewhere.[36] Briefly, solutions of pure phospholipids in $CHCl_3$ were dried and evaporated in round-bottomed flasks under a nitrogen flow. The resulting lipid film on the wall of the flask was hydrated with an appropriate volume of buffer and dispersed by vigorous stirring in a water bath set at 4 °C above the gel−liquid-crystal transition temperature of the membrane. The final nominal concentration of the lipid was 200 μM. To obtain large unilamellar vesicles (LUVs), the multilamellar vesicles (MLVs) so obtained were extruded through polycarbonate filters (pore size = 100 nm) (Nuclepore, Pleasanton, CA, U.S.) placed in a mini-extruder (Avestin Inc.) fitted with two 0.5 mL Hamilton gastight syringes (Hamilton, Reno, NV, U.S.). Typically, we subjected samples to 19 passes through two filters in tandem.

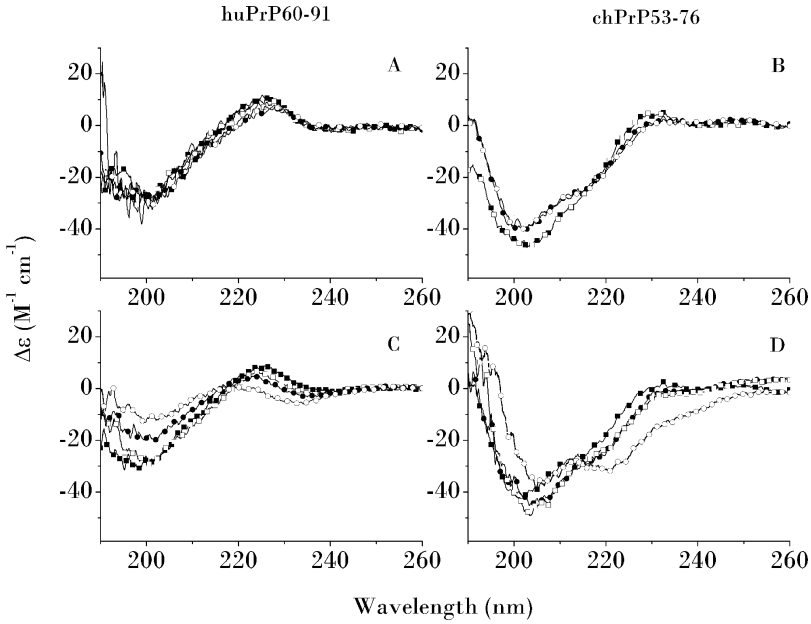

Figure 1. CD spectra of huPrP60-91 (A) and chPrP53-76 (B) in H_2O at different pH values (pH 4 = ■, pH 7 = □, pH 9 = ●, pH 11 = ○). CD spectra of huPrP60-91 (C) and chPrP53-76 (D) at neutral pH and different percentages of TFE (0% TFE = ■, 40% TFE = □, 80% TFE = ●, 100% TFE = ○).

Incorporation of huPrP60-91 and chPrP53-76 in Model Membranes. A proper amount of peptide solution in 25 mM NEM buffer was added to previously prepared DPPC LUV suspensions and analyzed at different times. The peptide/lipid ratio was kept fixed at 3/20 in all experiments. The copper(II) complexes with the investigated peptides were prepared at four different M/L molar ratios 1:1, 1:2, 1:3, and 1:4 and incubated with DPPC LUVs. The DSC, CD, or fluorescence experiment runs were performed immediately after peptide addition to the LUVs and at different incubation times up to a maximum of 48 h.

Differential Scanning Calorimetry. The DSC scans were carried out using a VP Microcal nano differential scanning calorimeter. The sampling rate was 1 point/s in all measuring ranges. The buffer solution without the sample was used in the reference cell. Both the sample and reference were heated with a precision of 0.05 °C at a scanning rate of 0.5 °C/min. To obtain the excess heat capacity ($C_{p,\mathrm{exc}}$) curves, buffer−buffer base lines were recorded at the same scanning rate and subtracted from the sample curve. A calibration of the energy was obtained by providing a definite power supply, electrically generated by a built-in calibrator within the sample cell. Three different samples were analyzed to check the reproducibility of the results. Control experiments were also carried out on the DPPC/Cu(II) systems in 25 mM NEM buffer at a Cu(II) concentration of 120 μM to rule out any possible effect of Cu(II) ions on the DSC curves of the membranes.

Circular Dichroism. The CD spectra were obtained at 25 °C under a constant flow of nitrogen on a JASCO model J-810 spectropolarimeter, calibrated with an aqueous solution of (1*R*)-(−)-10-camphorsulfonic acid, ammonium salt.[37] The CD measurements were carried out under a variety of experimental conditions, including different pH levels, peptide/Cu^{2+} molar ratios, and percentages of TFE, SDS, and DPC concentrations and the presence of DPPC LUV model membranes. The CD spectra were recorded in the UV region (190−260 nm) using 1 cm or 10 mm path length cuvettes. The peptide concentrations ranged from 5 to 30 μM. The spectra represent the average of 8−20 scans. The CD intensities are expressed as $\Delta\varepsilon$ (M^{-1} cm^{-1}). All CD measurements were repeated at different times up to a maximum of 48 h.

Fluorescence Spectroscopy. Fluorescence spectra were recorded with a Varian Cary Eclipse spectrofluorometer. Measurements were made in l cm path length cells in a volume of 1.00 mL. Fluorescence was excited at λ_{ex} = 280 nm and the emitted light recorded from 290 to 500 nm. Excitation and emission slits were fixed at 5 nm. The temperature of the solutions was maintained at 25.0 °C by circulating water through the jacket of the fluorescence cell holder. During the measurements the fluorescence spectrometer was checked for instrumental drift using either a solution of tryptophan in water or a reference buffer solution. Solvent blanks were run for each sample and were subtracted from the spectra.

Results

Conformational Preferences of huPrP60-91 and chPrP53-76 in Aqueous Solutions. The aqueous solution CD spectra of huPrP60-91 (Figure 1A) are characterized by a negative ellipticity centered at 200 nm and a weakly positive dichroic activity at 227 nm. These spectral features are similar to those reported for the type II poly-L-proline left-handed extended helix (PPII).[38] However, the negative CD band observed at around 200 nm suggests that the peptide may adopt two coexisting conformational states: type II poly-L-proline and a random coil.[24] As shown in Figure 1A, the CD curves were poorly affected by pH changes. The CD spectra recorded beyond pH 7.0 are characterized by a slight decrease in the positive ellipticity at 227 nm accompanied by a slight shift of the negative signal at 200 nm toward lower wavelength values. Although these spectral changes are small, they still suggest an increase of the amount of random coil conformations at basic pH values. This finding can be reconciled with the expected destabilizing effect of the four deprotonated hystidyl side chains on the PPII conformation.[24] Conversely, the CD spectra of chPrP53-76 in aqueous solutions, as shown in Figure 1B, suggest the coexistence of β-turn structures and random coil conformations, in agreement with previously reported results.[33]

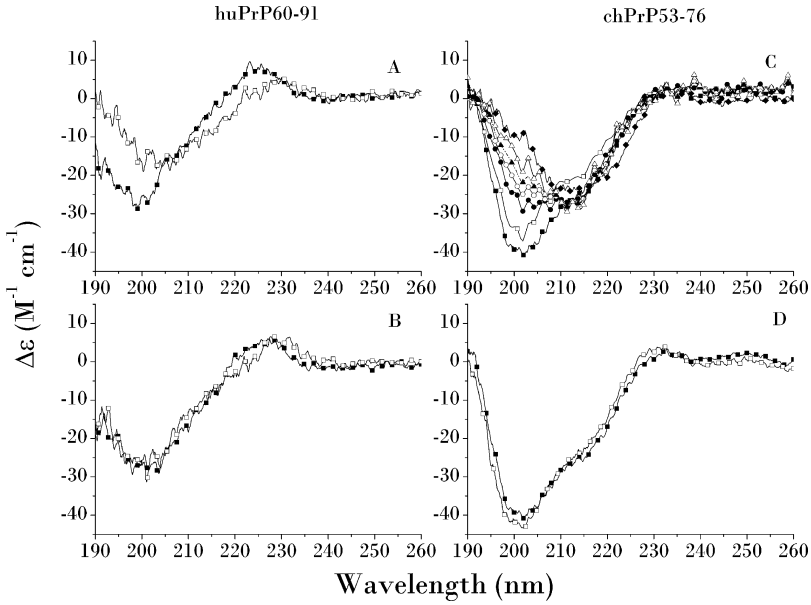

Figure 2. CD spectra of huPrP60-91 at pH 7 and at different concentrations of SDS (A; 0.1 mM = ■, 170 mM = □) and DPC (B; 1.0 mM = ■, 20 mM = □). Curves obtained at intermediate concentrations are not reported. CD spectra of chPrP53-76 at pH 7 and at different concentrations of SDS (C; 0.1 mM = ■, 0.5 mM = □, 1.0 mM = ●, 10 mM = ○, 20 mM = ▲, 100 mM = Δ, 170 mM = ◆) and DPC (panel D; 1.0 mM = ■, 20 mM = □). Curves obtained at intermediate concentrations are not reported.

Notably, the effect of pH changes on the conformational features of chPrP53-76 are more pronounced than the ones observed with huPrP60-91. In particular, when the coexistence of random coils and β-turn structures at acid pH values is inferred from the CD spectra of chPrP53-76, the positive band at 190 nm and the shoulder found at 216 nm, indicative of β-turn-like conformations,[33] appear to be predominant at neutral and basic pH values.

Conformational Behavior of huPrP60-91 and chPrP53-76 in Membrane-Mimicking Media. To further investigate the conformational properties of huPrP60-91 and chPrP53-76 in conditions similar to those occurring near the lipid bilayer, we recorded the CD spectra in TFE (Figure 1C,D). This solvent, which has a lower dielectric constant than water, is widely used to mimic the hydrophobic environments of membranes.[24] An increase in the percentage of TFE in the aqueous huPrP60-91 samples is accompanied by a decrease in the amplitude of the whole spectrum (Figure 1C). At 100% TFE, the CD spectrum shows two negative bands at around 200 and 235 nm. It might be hypothesized that the decrease of the band at 200 nm is related to TFE-induced structuring effects within the polypeptide backbone, whereas the decrease in the maximum at 230 nm might be related to a concomitant destabilization of the type II poly-L-proline conformation. Notably, despite the high tendency of TFE to stabilize structures through the formation of intramolecular hydrogen bonds, the CD spectrum of huPrP60-91 recorded at 100% TFE does not show any spectral feature of the α-helix conformation.[39–42] Conversely, the CD spectrum observed is more compatible with a reverse β-turn conformation in agreement with the CD spectra of huPrP55-98 obtained in 70% TFE.[43] The high propensity of chPrP53-76 to adopt β-turn structures in aqueous solution is confirmed by the CD spectra carried out at different TFE percentages (Figure 1D). The spectral features observed on increasing amounts of this solvent show only slight variations with a shift of the negative band toward 205 nm and the presence of a shoulder at 215 nm. Unlike those reported for huPrP60-91, the CD spectra of chPrP53-76 recorded at 100% TFE show well-defined spectral features, with a positive signal around 190 nm along with two negative bands at 206 and 220 nm. Such a CD profile may be assigned to a predominant type I β-turn (α-helix like) conformation.[44]

Circular dichroism studies were carried out either in anionic SDS or in neutral DPC detergents to further examine the roles played by electrostatic forces in driving the conformational properties of huPrP60-91 and chPrP53-76 in membrane-like environments. The CD spectra of huPrP60-91 carried out in SDS solutions below the critical micellar concentration (cmc, 1−10 mM) and at neutral pH were very similar to those recorded in aqueous solution.[45] An increase of the SDS concentration above the cmc (10.0−170 mM) resulted in stabilization of the type II poly-L-proline conformation, as indicated by the decrease in the negative ellipticity around 200 nm and its slight shift toward higher wavelength values (Figure 2A).

Unlike with the SDS, the CD spectra recorded at different concentrations of DPC (Figure 2B) did not change either below or above the cmc value of DPC (1 mM).[25] Thus, it may be argued that the SDS/huPrP60-91 interaction is aided by attractive electrostatic forces of the SDS's sulfate group and the ionizable His side chains with a consequent effect on the conformational properties of the peptide. On the other hand, the SDS micelles had a concentration-dependent effect on the conformation of chPrP53-76 as indicated both by the decrease in the minimum of the negative CD band at 200 nm and by the presence of a negative band at 216 nm (Figure 2C). Similar to that observed for huPrP60-91, the CD spectrum of chPrP53-76 recorded in the presence of DPC micelles (Figure 2D) at pH 7.0 is almost identical to the CD curves observed in aqueous solutions.

Conformational Properties of huPrP60-91 and chPrP53-76 in the Presence of Copper(II) Ions. It is known that avian and mammalian N-terminal repeats exhibit different copper(II) coordination modes in aqueous solution.[29,45–48] To explore the differences in the conformational behavior of huPrP60-91 and chPrP53-76 upon copper(II) addition, we recorded the CD spectra of the copper(II) complexes with the two peptides at different metal to ligand (M/L) molar ratios. The CD experiments were also carried out in aqueous solutions or in different buffers to rule out any possible bias affecting copper(II) coordination to the peptides. In pure water and at pH 7.0 (Figure

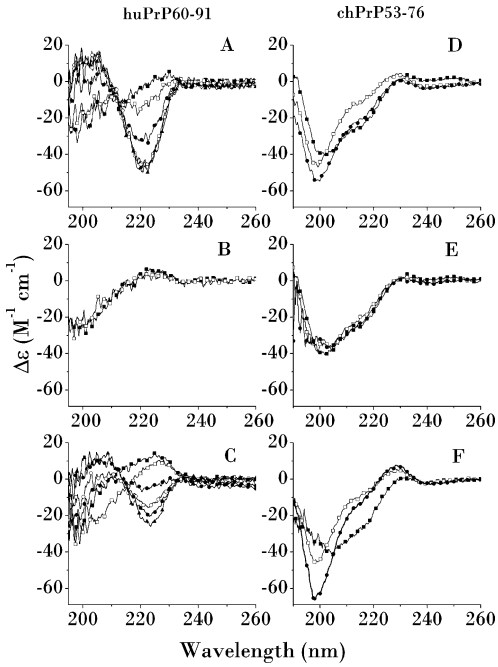

Figure 3. CD spectra of Cu(II)/huPrP60-91 systems at pH 7.0 and at different M/L ratios recorded in H_2O (A; M/L 0 = ■, M/L 1 = □, M/L 2 = ●, M/L 3 = ○, M/L 4 = ▲), 10 mM phosphate buffer (B; M/L 0 = ■, M/L 4 = □, intermediate curves not shown), and 25 mM NEM buffer (C; M/L 0 = ■, M/L 1 = □, M/L 2 = ●, M/L 3 = ○, M/L 4 = ▲). CD spectra of Cu(II)/chPrP53-76 systems at pH 7.0 and at different M/L ratios recorded in H_2O (D; M/L 0 = ■, M/L 1 = □, M/L 2 = ●), 10 mM phosphate buffer (E; M/L 0 = ■, M/L 1 = □, M/L 2 = ●), 25 mM NEM buffer (C; M/L 0 = ■, M/L 1 = □; M/L 2 = ●).

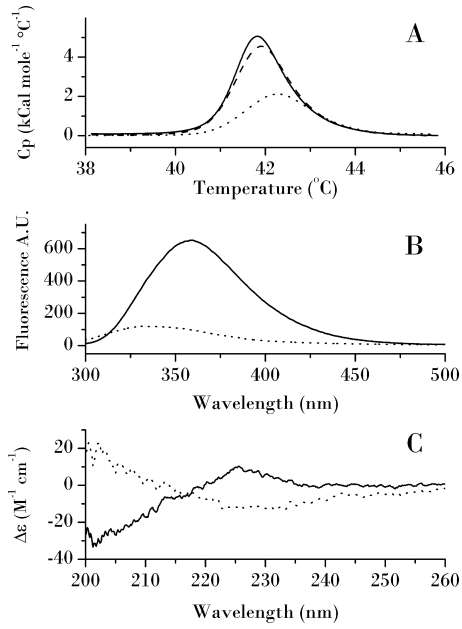

Figure 4. (A) DSC curves of pure DPPC (solid line) and DPPC/huPrP60-91 recorded immediately after peptide addition (dashed line) and after 30 h (dotted line). (B) Trp fluorescence emission spectra (λ_{ex} = 280 nm, excitation and emission slits 5 nm, range 300−500 nm) of DPPC/huPrP60-91 recorded immediately after peptide addition (solid line) and after 30 h (dashed line). (C) CD spectra of DPPC/huPrP60-91 recorded immediately after peptide addition (solid line) and after 30 h (dashed line). All the experiments were carried out under the following conditions: pH 7.0 in 25 mM NEM buffer, C_{DPPC} = 200 μM, $C_{huPrP60-91}$ = 30 μM.

3A), the Cu^{2+} induced evident conformational changes in huPrP60-91. At high M/L ratios, a negative dichroic band around 220 nm is observed; the concomitant formation of a positive maximum at about 200 nm indicates that Cu^{2+} coordination induces peptide backbone structuring in a β-turn conformation.

Conversely, in 10 mM phosphate buffer no changes in the CD profiles were observed at any of the M/L ratios investigated (Figure 3B). This suggests that phosphate competes with huPrP60-91 for the binding to Cu^{2+}. Since it has been reported that morpholine-based buffers do not interact with Cu^{2+},[49] we performed CD experiments in a 25 mM NEM buffer at pH 7.0 (Figure 3C). Titrations of huPrP60-91 in the NEM buffer with increasing amounts of Cu^{2+} indicated conformational changes similar to those observed in pure water, confirming that this buffer is not competitive for the binding to Cu^{2+}. The effect of Cu^{2+} binding on the conformational equilibria of chPrP53-76 was also explored using a 1:1 and a 2:1 M/L ratio, for comparison, at pH 7.0 in water (Figure 3D), in agreement with previously reported data.[29] The addition of 1 equiv of Cu^{2+} induced a slight variation in the peptide conformation upon copper(II) binding, with the negative band around 203 nm blue shifting toward 198 nm and significantly increasing in intensity. A similar effect was observed for the signal at 230 nm, which shifted at 228 and increased in intensity, whereas a negative signal appeared at 240−250 nm, suggesting the involvement of histidine residues in Cu^{2+} complexation. The addition of a second Cu^{2+} equivalent induced a decrease of the negative band at 198 nm and an increase of the positive band at 228 nm. The addition of increasing amounts of Cu^{2+} (more than 2 equiv) to the chPrP53-76 at a neutral pH was also attempted, but it caused peptide precipitation, as previously observed.[29] When phosphate buffer was used (Figure 3E), no changes in the CD spectra of chPrP53-76 were observed upon Cu^{2+} addition, which was similar to the experiment with huPrP60-91. Titrations of chPrP53-76 in the NEM buffer (Figure 3F) indicated changes in the CD spectra similar to those observed in water, confirming again that this buffer does not compete for Cu^{2+} binding.

Interactions of huPrP60-91, chPrP53-76, and Their Cu(II) Complexes with DPPC Model Membranes. The potential of DSC experiments to provide useful information concerning peptide/membrane interactions relies on the fact that heat capacity (Cp) profiles of the main transitions of mixed lipid/peptide systems can help to clarify not only the effects of the peptide on the membrane but also the topological arrangement of the peptide when it is inserted into the lipid matrix. In fact, the enthalpy variations observed during the main lipid transitions are mainly ascribable to the efficiency in the packing of the hydrocarbon tail.[50] It is thus possible to relate the peptide-induced decrease of the transition enthalpy of the bilayer to the extent of the interactions between guest molecules and the core of lipid membranes. Moreover, the main transition temperature (T_m) is more sensitive to interactions involving the lipid headgroups, increasing when the membrane surface is involved in the interaction with the guest peptide.[51–53] The DSC profiles the of DPPC/huPrP60-91 system recorded immediately after the sample preparation (dashed line) and at 30 h of incubation (dotted line) are illustrated in Figure 4.

The DSC curve of pure DPPC large unilamellar vesicles (LUVs) (solid line) is also shown for comparison. These calorimetric profiles show that the thermal transition of DPPC membranes incubated with huPrP60-91 is noticeably affected after 30 h. In particular, the presence of huPrP60-91 reduced the transition enthalpy from 8.5 ± 0.3 to 4.3 ± 0.3 kcal mol^{-1} ($\Delta\Delta H$ = −4.2 kcal mol^{-1}) and the temperature of transition was slightly increased from T_m = 41.8 ± 0.1 °C to T_m = 42.3

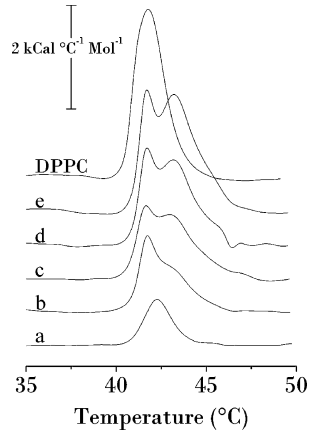

Figure 5. DSC curves of Cu(II)/DPPC/huPrP60-91 mixtures obtained at different metal to ligand ratios and recorded after 30 h incubation. The first curve represents the DSC profile of pure DPPC LUVs. Curve a represents the DSC profile of the DPPC/huPrP60-91 system. Curves b−e represent the DSC profile of the Cu(II)/DPPC/huPrP60-91 system at 1:1, 2:1, 3:1, and 4:1 metal to peptide ratios, respectively. All the experiments were carried out under the following conditions: pH 7.0 in NEM buffer, $C_{DPPC} = 200\ \mu M$, $C_{huPrP60-91} = 30\ \mu M$.

$\pm$ 0.1 °C ($\Delta T_m = +0.6$ °C). Taken together, the DSC results indicate a slow, spontaneous insertion of the peptide into the hydrocarbon core of the membrane. The time-dependent insertion of huPrP60-91 into the lipid matrix was also monitored by Trp fluorescence emission measurements. The emission spectra of the tryptophan residues were recorded throughout the incubation of huPrP60-91 with DPPC. After 30 h incubation, a blue shift of the emission peak from 354 nm (Figure 4B, solid line) to 330 nm (Figure 4B, dotted line) was observed. This blue shift indicates a change in the environment surrounding the tryptophan residues of huPrP60-91 from an aqueous to a hydrophobic situation, thereby suggesting an insertion of these residues into the lipid core of the membrane. Moreover, changes in the emission spectra were also accompanied by a significant reduction in emission intensity, which may reflect a structural reorganization of the peptide.[54,55] The structural peptide reorganization, which accompanies the membrane interaction, was further monitored by CD experiments carried out after 30 h incubation with the DPPC vesicles. These CD profiles showed a positive ellipticity at 200 nm and a negative ellipticity at 230 nm, suggesting a β-sheet conformation. Additional experiments carried out at different incubation times for up to 48 h showed that the lipid/peptide interaction was maximal after 30 h (data not shown). To investigate the effect of Cu^{2+} in modulating the lipid/peptide interaction, we used the same experimental approach as reported for the metal-free peptides. The DSC profiles of DPPC after 30 h incubation with huPrP60-91 (curve a) and preformed copper(II) complexes with huPrP60-91 at different metal to ligand molar ratios (curves b−e) are illustrated in Figure 5.

The DSC curve of pure DPPC LUVs is also shown for comparison. Incubation with Cu^{2+} and huPrP60-91 at a 1:1 ratio (curve b) induced a less severe membrane destabilization but two shoulders appear at $T_m = 41.8$ °C and $T_m = 43.1$ °C, suggesting the existence of phase segregation phenomena.[56] All of the DSC curves obtained after incubating the DPPC LUVs with huPrP60-91 and at 1:1, 1:2, 1:3, and 1:4 Cu^{2+} to huPrP60-91 ratios revealed that phase segregation was more evident at increasing M/L ratios (curves b−e). The two unresolved peaks in the DSC thermograms are due to a nonuniform distribution of metal complex species in the bilayer. In particular, the appearance of the shoulder located at the high-temperature side of the thermogram could be ascribed to the segregation of a group of "boundary" lipid molecules surrounding the copper(II) complex. Incubating the preformed metal complexes with DPPC membranes did not affect the conformational features of the metal complexes (data not shown). On the other hand, the addition of increasing amounts of Cu^{2+} to preincubated lipid/peptide mixtures did not modify the DSC profiles of DPPC/huPrP60-91 systems, thus demonstrating that insertion of the peptide into the lipid matrix cannot be reversed upon Cu^{2+} addition. These results imply that the metal coordination modes are not modified upon membrane binding and, conversely, that in the membrane-bound peptide the Cu^{2+} anchoring amino acid residues are buried in the lipid interior and are not accessible to copper(II) ions. In striking contrast to huPrP60-91, the DSC profiles of the DPPC/chPrP53-76 system recorded immediately or after 30 h of incubation showed a similar thermal transition of pure DPPC membranes, indicating the absence of any peptide/membrane interactions even after 30 h of incubation. The same measurements carried out after Cu^{2+} addition (one and two equivalents) showed identical DSC profiles of the pure DPPC membrane even after 30 h of coincubation (data not shown).

Discussion

It is widely recognized that environmental factors, e.g., pH changes, membranes, and copper(II) ions, may play a relevant role either in PrP functioning or in its pathogenic conversion. Specifically, aberrant variations in the biophysical features of the N-terminal domain are believed to influence the structural conversion and aggregation of PrP that take place during prion propagation. In spite of these tantalizing clues, comparative studies of avian and human PrP N-terminal domains regarding their conformational behavior and membrane activity under different environmental conditions are not currently available.

In the present work we confirmed that the structural features of huPrP60-91 in aqueous solution may be described as a mixture of random coils and PPII structures, an equilibrium poorly affected by pH. It is noteworthy that unlike α-helices and β-sheets, there are no characteristic main-chain hydrogen-bonding patterns in PPII structures, making them very difficult to detect by NMR or X-ray spectroscopy.[57] Consequently, PPII helices are often assigned as unstructured or random coils in aqueous solution. However, far-UV-CD spectra of PPII and random coil structures have distinct signatures, thus helping to distinguish between these two conformations. Furthermore, very recent NMR results obtained at acidic pH values have confirmed that the N-terminal domain of the prion protein displays the contemporary presence of PPII, random coils, and β-turn conformations.[58]

Different membrane-mimicking environments, i.e., negatively charged (SDS) or zwitterionic (DPC) micelles and water/TFE mixtures, were found to induce different conformational changes to huPrP60-91. In particular, increasing amounts of TFE induce a conformational transition toward reverse β-turn structures in huPrP60-91, even though this conformation coexists with the PPII structure. Nonetheless, negatively charged SDS micelles induce a stabilization of the PPII structure. These different effects of TFE and SDS on the conformation of huPrP60-91 may be explained by considering the different physicochemical properties of the two systems. Despite the fact that both TFE and SDS are widely used to mimic the membrane environment, TFE is known to promote the formation of intramolecular hydrogen bonds, thereby inducing peptides to adopt internally H-bonded structures similar to those observed in the CD

spectra.[59–64] This effect is not observed in SDS micelles where the different dielectric constant of water is known to stabilize PPII structures.[65] Indeed, another important difference existing between TFE and SDS membrane mimicking environments relies on the fact that SDS micellar systems are dispersed in water; thus, our results are consistent with the essential role of hydration in stabilizing the conformation of PPII. The CD spectra of huPrP60-91 in DPC micelles were almost indistinguishable from those observed in pure water. This result underlines the importance of electrostatic interactions in stabilizing PPII structures.

The Trp fluorescence, CD, and DSC experiments carried out on peptide/DPPC systems indicate a slow insertion of the peptide into the hydrocarbon core of the zwitterionic membrane. According to the Trp fluorescence experiments, the DPPC/peptide interactions mainly occur through the hydrophobic Trp residues and force the peptide to reorganize its structure. The structural peptide reorganization that accompanies the membrane interaction was monitored by CD experiments that showed significant changes in the shape of the CD spectra. All these results concur to support the hypothesis that both Cu^{2+} and the membrane-like environment may induce significant modifications to the structure of huPrP60-91. In fact, upon Cu^{2+} addition, huPrP60-91 adopts a β-turn structure that has been ascribed to a His-Trp interaction occurring at high metal/ligand ratios.[66] Conversely, the CD spectra of huPrP60-91 added to the DPPC membranes are suggestive of extended β-sheet-like peptides. These results match with thermodynamic models showing that the driving force of the incorporation of a peptide into the membrane generally acts against the unfavorable free-energy cost of inserting the peptide bonds into the hydrocarbon core.[67] However, if the peptide in the lipid matrix adopts a conformation that can reduce this high free-energy cost, the incorporation of a peptide into the membrane becomes favored. Furthermore, membrane-driven modifications are very slow (about 36 h) when compared to the conformational changes induced by Cu^{2+}, probably because of the high viscosity of the lipid medium. The minor conformational changes as a consequence of adding SDS or DPC micelles suggest that the ordered hydrophobic environment provided by the lipid bilayer is the major driving force in promoting the interaction of huPrP60-91 with the membrane and, consequently, in modulating the conformational properties of the peptide. Membrane interactions of copper(II) complexes with huPrP60-91 were shown to depend on the number of Cu^{2+} ions bound to the peptide. In fact, DSC experiments have shown that the enthalpy of the main transition of the membrane after incubation with a 4:1 preformed metal/peptide complex is similar to that observed for the pure lipid; however, the DSC profiles assume a complex shape with at least two separate peaks. It is likely that Cu^{2+} binding enhances huPrP60-91 conformational rigidity with a consequent decrease in the ability of the peptide to be accommodated in the hydrophobic environment of the membrane. Indeed, it is known that the octarepeat domain of huPrP, at neutral pH levels, passes through a series of distinct binding modes as a function of the Cu^{2+}/peptide ratio.[46] At high Cu^{2+} occupancy, i.e., from 2 to 4 equiv of metal ions, a component is predominant in which the coordination environment of copper(II) is constituted by the His imidazole, two deprotonated amide nitrogens from the two following Gly residues and an axial water molecule that bonds to the NH of the Trp indole. In a second component, which predominates at 1 or 2 Cu^{2+} equivalents, a N_2O_2 (N_{im}, N^-, $2H_2O$) coordination mode is present. Consequently, although coexistence of the two components at an intermediate metal ion occupancy cannot be ruled out, an increase of the Cu^{2+}/peptide ratio is expected to shift the equilibrium toward the first component in which the Trp indole is involved in the copper(II) coordination sphere. It should be pointed out that the binding of the axial water molecule that interacts with the Trp indole in the component predominant at high Cu^{2+} occupancy has been questioned elsewhere.[68] In particular, the involvement of a carbonyl oxygen atom in the metal coordination has been proposed. In both hypotheses, on increasing copper(II) concentrations, the Trp residue shows a tendency to approach the copper center, thus becoming less available to an interaction with the membrane. Furthermore, EPR studies have revealed dipolar couplings arising from proximal copper(II) ions, suggesting that the octarepeat domain undergoes a partial hydrophobic collapse upon Cu^{2+} addition.[46] Such a collapse is also likely to hinder a tight interaction of Trp with the lipid bilayer. This view fully agrees with the data presented herein, thus providing a reasonable picture of the interplay existing between copper(II) occupancy, availability of the hydrophobic Trp moiety and extent of insertion of the peptide into the lipid bilayer. Our results suggest that the structure and the coordination of the copper(II) binding sites of the N-terminal region of human PrP may play a critical role in modulating PrP interactions with membranes.

The comparative experiments carried out on chPrP53-76 showed that both the metal-free and the copper(II)-bound peptide do not show any tendency to interact with zwitterionic membranes even after prolonged incubation. This remarkable difference between chPrP53-76 and hPrP60-91 can be explained by considering the diverse contents of Gly and Pro residues in their primary sequences. The mammalian octarepeat peptides contain 50% glycine and 12% proline residues, while the chicken hexarepeats contain 16% glycine and 33% proline residues. The higher number of glycine residues results in the greater flexibility of huPrP60-91 and might explain its propensity to promote polyproline conformations together with unordered structures. On the contrary, the high number of proline residues can explain the tendency of avian hexarepeats to form β-turn structures, also driven by tyrosine residues. There is no tryptophan residue in the primary sequence of avian tandem repeats and these results further support the main role of this residue in driving membrane interactions. Moreover chPrP53-76 is known to bind no more than two copper(II) equivalents and the predominant copper(II) complex species (at any metal to ligand ratio) was always $CuLH_4$, corresponding to a metal ion bound to four imidazole nitrogen atoms in a plane.[29] The huPrP60-91 forms an analogous copper(II) complex species but it is predominant only in a low metal to ligand molar ratio (less than 1 equiv).[46] This is in agreement with the finding that the phase segregation of the copper(II)/huPrP60-91 system is more evident at increasing amounts of metal ions, corresponding to the formation of complex species involving the amide nitrogen atoms of the peptide backbone and then with the formation of β-turn structures. All the data obtained on huPrP60-91, coupled with the different conformational behaviors and the reduced copper(II) binding ability of the avian peptide, support the hypothesis that the N-terminal regions of human and chicken prion proteins are involved in different physiological functions of prions and may play roles in differentiating their processing within the cell.

Acknowledgment. This work was financially supported by Consiglio Nazionale delle Ricerche (RSTL no. 620), Università di Catania (Progetti di Ateneo 2008), and MIUR (PRIN2006-033492, FIRB RBNEO3PX83_001, and RBPR05JH2P_021).

References and Notes

(1) Prusiner, S. B. Prions. *Proc. Natl. Acad. Sci. U.S.A.* **1998**, *95*, 13363–13383.

(2) Prusiner, S. B. *Prion Biology and Diseases*, 2nd ed.; Prusiner, S. B., Ed.; Cold Spring Harbor Laboratory Press: Cold Spring Harbor, NY, U.S., 2004.

(3) Prusiner, S. B. Prion Diseases and the BSE Crisis. *Science* **1997**, *278*, 245–251.

(4) Zahn, R.; Liu, A.; Luhrs, T.; Riek, R.; von Schroetter, C.; Garcia, F. L.; Billeter, M.; Calzolai, L.; Wider, G.; Wüthrich, K. NMR solution structure of the human prion protein. *Proc. Natl. Acad. Sci. U.S.A.* **2000**, *97*, 145–150.

(5) Donne, D. G.; Viles, J. H.; Groth, D.; Mehlhorn, I.; James, T. L.; Cohen, F. E.; Prusiner, S. B.; Wrigth, P. E.; Dyson, H. J. Structure of the recombinant full-length hamster prion protein PrP (29−231): The N terminus is highly flexible. *Proc. Natl. Acad. Sci. U.S.A.* **1997**, *94*, 13452–13456.

(6) Zahn, R. The octapeptide repeats in mammalian prion protein constitute a pH-dependent folding and aggregation site. *J. Mol. Biol.* **2003**, *334*, 477–488.

(7) Govaerts, C.; Wille, H.; Prusiner, S. B.; Cohen, F. E. Evidence for assembly of prions with left-handed β-helices into trimers. *Proc. Natl. Acad. Sci. U.S.A.* **2004**, *101*, 8342–8347.

(8) Wille, H.; Michelitsch, M. D.; Guenebaut, V.; Supattapone, S.; Serban, A.; Cohen, F. E.; Agard, D. A.; Prusiner, S. B. Structural studies of the scrapie prion protein by electron crystallography. *Proc. Natl. Acad. Sci. U.S.A.* **2002**, *99*, 3563–3568.

(9) Harris, D. A.; Falls, D. L.; Johnson, F. A.; Fischbach, G. D. A prion-like protein from chicken brain copurifies with an acetylcholine receptor-inducing activity. *Proc. Natl. Acad. Sci. U.S.A.* **1991**, *88*, 7664–7668.

(10) Schätzl, H. M.; Da Costa, M.; Taylor, L.; Cohen, F. E.; Prusiner, S. B. Prion protein gene variation among primates. *J. Mol. Biol.* **1995**, *245*, 362–374.

(11) Calzolai, L.; Lysek, D. A.; Perez, D. R.; Guntert, P.; Wüthrich, K. Prion protein NMR structures of chickens, turtles, and frogs. *Proc. Natl. Acad. Sci. U.S.A.* **2005**, *102*, 651–655.

(12) Pietropaolo, A.; Muccioli, L.; Zannoni, C.; Rizzarelli, E. Conformational preferences of the Full Chicken Prion Protein in solution and its differences with respect to mammals. *Chem. Phys. Chem.* **2009**, *10*, 1500–1510.

(13) Marcotte, E. M.; Eisemberg, D. Chicken Prion Tandem Repeats Form a Stable, Protease-Resistant Domain. *Biochemistry* **1999**, *38*, 667–676.

(14) Matthews, D.; Cooke, B. C. The potential for transmissible spongiform encephalopathies in non-ruminant livestock and fish. *Rev. Sci. Technol.* **2003**, *22*, 283–96.

(15) Millhauser, G. L. Copper binding in the prion protein. *Acc. Chem. Res.* **2004**, *37*, 79–85.

(16) Vassallo, N.; Herms, J. Cellular prion protein function in copper homeostasis and redox signalling at the synapse. *J. Neurochem.* **2003**, *86*, 538–544.

(17) Miura, T.; Sasaki, S.; Toyama, A.; Takeuchi, H. Copper Reduction by the Octapeptide Repeat Region of Prion Protein: pH Dependence and Implications in Cellular Copper Uptake. *Biochemistry* **2005**, *44*, 8712–8720.

(18) Daniels, M.; Brown, D. R. Purification and preparation of prion protein: The synaptic superoxide dismutase. *Methods Enzymol.* **2002**, *349*, 258–267.

(19) Pauly, P. C.; Harris, D. A. Copper Stimulates Endocytosis of the Prion Protein. *J. Biol. Chem.* **1998**, *273*, 33107–33119.

(20) Taylor, D. R.; Watt, N. T.; Sumudhu, W.; Perera, S.; Hooper, N. M. Assigning functions to distinct regions of the N-terminus of the prion protein that are involved in its copper-stimulated, clathrin-dependent endocytosis. *J. Cell Sci.* **2005**, *118*, 5141–5153.

(21) Klein, T. R.; Kirsch, D.; Kaufmann, R.; Riesner, D. Prion rods contain small amounts of two host sphingolipids as revealed by thin-layer chromatography and mass spectrometry. *Biol. Chem.* **1998**, *379*, 655–666.

(22) Morillas, M.; Swietnicki, W.; Gambetti, P.; Surewicz, W. K. Membrane Environment Alters the Conformational Structure of the Recombinant Human Prion Protein. *J. Biol. Chem.* **1999**, *274*, 36859–36865.

(23) Miura, T.; Yoda, M.; Takaku, N.; Hirose, T.; Takeuchi, H. Clustered Negative Charges on the Lipid Membrane Surface Induce β-Sheet Formation of Prion Protein Fragment 106−126. *Biochemistry* **2007**, *46*, 11589–11597.

(24) Smith, C. J.; Drakeb, A. F.; Anfield, B. A.; Bloomberga, G. B.; Palmerc, M. S.; Clarkea, A. R.; Collinge, J. Conformational properties of the prion octa-repeat and hydrophobic sequences. *FEBS Lett.* **1997**, *405*, 378–384.

(25) Dong, S. L.; Cadamuro, S. A.; Fiorino, F.; Bertsch, U.; Moroder, L.; Renner, C. Copper binding and conformation of the N-terminal octarepeat of the prion protein in the presence of DPC micelles as membrane mimetic. *Biopolymers* **2007**, *88*, 840–847.

(26) Berti, F.; Gaggelli, E.; Guerrini, R.; Janicka, A.; Kozlowski, H.; Legowska, A.; Miecznikowska, H.; Migliorini, C.; Pogni, R.; Remelli, M.; Rolka, K.; Valensin, D.; Valensin, G. Structural and dynamic characterization of copper(II) binding of the human prion protein outside the octarepeat region. *Chem.−Eur. J.* **2007**, *13*, 1991–2001.

(27) Burns, C. S.; Aronoff-Spencer, E.; Legname, G.; Prusiner, S. B.; Antholine, W. E.; Gerfen, G. J.; Peisach, J.; Millhauser, G. L. Copper coordination in the full-length, recombinant prion protein. *Biochemistry* **2003**, *42*, 6794–6803.

(28) La Mendola, D.; Pietropaolo, A.; Pappalardo, G.; Zannoni, C.; Rizzarelli, E. Prion proteins leading to neurodegeneration. *Curr. Alzheimer Res.* **2008**, *5*, 579–590. Erratum. *Curr. Alzheimer Res.* **2009**, *6*, 321.

(29) La Mendola, D.; Bonomo, R. P.; Caminati, S.; Di Natale, G.; Emmi, S. S.; Hansson, Ö.; Maccarrone, G.; Pappalardo, G.; Pietropaolo, A.; Rizzarelli, E. Copper(II) complexes with an avian prion N-terminal region and their potential SOD-like activity. *J. Inorg. Biochem.* **2009**, *103*, 195–204.

(30) Valensin, D.; Luczkowski, M.; Mancini, F. M.; Legowska, A.; Gaggelli, E.; Valensin, G.; Rolka, K.; Kozlowski, H. The dimeric and tetrameric octarepeat fragments of prion protein behave differently to its monomeric unit. *Dalton Trans.* **2004**, 1284–1293.

(31) Di Natale, G.; Grasso, G.; Impellizzeri, G.; La Mendola, D.; Micera, G.; Mihala, N.; Nagy, Z.; Osz, K.; Pappalardo, G.; Rigo, V.; Rizzarelli, E.; Sanna, D.; Sovago, I. Copper(II) interaction with unstructured prion domain outside the octarepeat region: speciation, stability and binding details of copper(II) complexes with PrP106−126 peptides. *Inorg. Chem.* **2005**, *44*, 7214–7125.

(32) Gralka, E.; Valensin, D.; Gajda, K.; Bacco, D.; Szyrwiel, L.; Remelli, M.; Valensin, G.; Kamasz, W.; Baranska-Rybak, W.; Kozlowski, H. Copper(II) coordination outside the tandem repeat region of an unstructured domain of chicken prion protein. *Mol. Biosyst.* **2009**, *5*, 497–510.

(33) Pietropaolo, A.; Muccioli, L.; Zannoni, C.; La Mendola, D.; Maccarrone, G.; Pappalardo, G.; Rizzarelli, E. Unveiling the role of histidine and tyrosine residues on the conformation of the avian prion hexarepeat domain. *J. Phys. Chem. B* **2008**, *112*, 5182–5188.

(34) Di Natale, G.; Impellizzeri, G.; Pappalardo, G. Conformational properties of peptide fragments homologous to the 106−114 and 106−126 residues of the human prion protein: a CD and NMR spectroscopicstudy. *Org. Biol. Chem.* **2005**, *3*, 490–497.

(35) Choi, G.; Guo, J.; Makriyannis, A. The conformation of the cytoplasmic helix 8 of the CB1 cannabinoid receptor using NMR and circular dichroism. *Biochim. Biophys. Acta* **2005**, *1668*, 1–9.

(36) Grasso, D.; Milardi, D.; La Rosa, C.; Rizzarelli, E. DSC study of the interaction of the prion peptide PrP106−126 with artificial membranes. *New J. Chem.* **2001**, *25*, 1543–1548.

(37) Chen, G. C.; Yang, J. T. Two-point calibration of circular dichrometer with d-10-camphorsulfonic acid. *Anal. Lett.* **1977**, *10*, 1195–1207.

(38) Tatham, A. S.; Drake, A. F.; Shewry, P. R. Conformational studies of a synthetic peptide corresponding to the repeat motif of C hordein. *Biochem. J.* **1989**, *259*, 471–476.

(39) Timasheff, S. N.; Susi, H.; Townend, R.; Stevens, L.; Gorbunoff, M. J.; Kumosinski, T. F. In *Conformation of Biopolymers*; Ramachandran, G. N., Ed.; Academic Press: London, 1967; Vol. 1.

(40) Drake, A. F.; Siligardi, G.; Gibbons, W. A. Reassessment of the electronic circular dichroism criteria for random coil conformations of poly(L-lysine) and the implications for protein folding and denaturation studies. *Biophys. Chem.* **1988**, *31*, 143–146.

(41) Brahms, S.; Brahms, J. Determination of protein secondary structure in solution by vacuum ultraviolet circular dischroism. *J. Mol. Biol.* **1980**, *138*, 149–178.

(42) Johnson, W. C., Jr. Protein secondary structure and circular dichroism: A practical guide. *Proteins Struct. Funct. Genet.* **1990**, *7*, 205–214.

(43) Leliveld, S. R.; Stitz, L.; Korth, C. Expansion of the octarepeat domain alters the misfolding pathway but not the folding pathway of the prion protein. *Biochemistry* **2008**, *47*, 6267–6278.

(44) Pietropaolo, A.; Raiola, L.; Muccioli, L.; Tiberio, G.; Zannoni, C.; Fattorusso, R.; Isernia, C.; La Mendola, D.; Pappalardo, G.; Rizzarelli, E. An NMR and Molecular Dynamics investigation of the avian prion hexarepeat conformational features in solution. *Chem. Phys. Lett.* **2007**, *442*, 110–118.

(45) Monserret, R.; Mc Leish, M. J.; Beckmann, A.; Geonzjann, C.; Penin, F. Involvement of Electrostatic Interactions in the Mechanism of Peptide Folding Induced by Sodium Dodecyl Sulfate Binding. *Biochemistry* **2000**, *39*, 8362–8373.

(46) Chattopadhyay, M.; Walter, E. D.; Newell, D. J.; Jackson, P. J.; Aronoff-Spencer, E.; Peisach, J.; Gerfen, G. J.; Bennett, B.; Antholine, W. E.; Millhauser, G. L. The octarepeat domain of the prion protein binds Cu(II) with three distinct coordination modes at pH 7.4. *J. Am. Chem. Soc.* **2005**, *36*, 12649–12656.

(47) Wells, M. A.; Jelinska, C.; Hosszu, L. L. P.; Craven, C. J.; Clarke, A. R.; Collinge, J.; Waltho, J. P.; Jackson, G. S. Multiple forms of copper

(II) co-ordination occur throughout the disordered N-terminal region of the prion protein at pH 7.4. *Biochem. J.* **2006**, *400*, 501–510.

(48) Viles, J. H.; Cohen, F. E.; Prusiner, S. B.; Goodin, D. B.; Wright, P. E.; Dyson, H. J. Copper binding to the prion protein: Structural implications of four identical cooperative binding sites. *Proc. Natl. Acad. Sci. U.S.A.* **1999**, *96*, 2042–2047.

(49) Dawson, R. M. C.; Elliott, D. C.; Elliott, W. H.; Jones, K. M. *Data for Biochemical Research*; Oxford University Press: Oxford, U.K., 1986.

(50) McDonald, R. C.; McDonald, R. I.; Menco, B. Ph. M.; Takeshita, K.; Subbarao, N. K.; Hu, L. Small-volume extrusion apparatus for preparations of large unilamellar vesicles. *Biochim. Biophys. Acta* **1991**, *1061*, 297–303.

(51) Sanderson, J. M. Peptide-lipid interactions: insights and perspectives. *Org. Biomol. Chem.* **2005**, *3*, 201–212.

(52) Nagle, J. F. Theory of the main lipid bilayer Phase Transition. *Annu. Rev. Phys. Chem.* **1980**, *31*, 157–195.

(53) Pappalardo, G.; Milardi, D.; Magrì, A.; Attanasio, F.; Impellizzeri, G.; La Rosa, C.; Grasso, D.; Rizzarelli, E. Environmental factors differently affect rat and human IAPP: conformational preferences and membrane activity of IAPP 17−29 peptide derivatives. *Chem.—Eur. J.* **2007**, *13*, 10204–10215.

(54) Alston, R. W.; Lasagna, M.; Grimsley, G. R.; Scholtz, J. M.; Reinhart, G. D.; Pace, C. N. Peptide sequence and conformation strongly influence tryptophan fluorescence. *Biophys. J.* **2008**, *94*, 2880–2887.

(55) Heyn, M. P.; Blume, A.; Rehorek, M.; Dencher, N. A. Calorimetric and fluorescence depolarization studies on the lipid phase transition of bacteriorhodopsin-dimyristoylphosphatidylcholine vesicles. *Biochemistry* **1981**, *20*, 7109–7115.

(56) Grasso, D.; Milardi, D.; Guantieri, V.; La Rosa, C.; Rizzarelli, E. Interaction of prion peptide PrP180−193 with DPPC model membranes: a thermodynamic study. *New J. Chem.* **2003**, *27*, 359–364.

(57) Chiang, Y. C.; Lin, Y. J.; Horng, J. C. Stereoelectronic effects on the transition barrier of polyproline conformational interconversion. *Protein Sci.* **2009**, *18*, 1967–1977.

(58) Taubner, L. M.; Bienkiewicz, E. A.; Copié, V.; Caughey, B. Structure of the flexible amino-terminal domain of prion protein bound to a sulfated glycan. *J. Mol. Biol.* **2010**, *395*, 475–490.

(59) Khemtemourian, L.; Sani, M. A.; Bathany, K.; Grobner, G.; Dufourc, E. J. Synthesis and secondary structure in membranes of the Bcl-2 anti-apoptotic domain BH4. *J. Pept. Sci.* **2006**, *12*, 58–64.

(60) Sonnichsen, F. D.; Van Eyk, J. E.; Hodges, R. S.; Sykes, B. D. Effect of trifluoroethanol on protein secondary structure: an NMR and CD study using a synthetic actin peptide. *Biochemistry* **1992**, *31*, 8790–8798.

(61) Santiveri, C. M.; Pantoja-Uceda, D.; Rico, M.; Jimenez, M. A. Beta-hairpin formation in aqueous solution and in the presence of trifluoroethanol: a 1H and 13C nuclear magnetic resonance conformational study of designed peptides. *Biopolymers* **2005**, *79*, 150–162.

(62) Calamai, M.; Chiti, F.; Dobson, C. M. Amyloid fibril formation can proceed from different conformations of a partially unfolded protein. *Biophys. J.* **2005**, *89*, 4201–4210.

(63) Pallares, I.; Vendrell, J.; Aviles, F. X.; Ventura, S. Amyloid fibril formation by a partially structured intermediate state of alpha-chymotrypsin. *J. Mol. Biol.* **2004**, *342*, 321–331.

(64) Shanmugam, G.; Polavarapu, P. L.; Gopinath, D.; Jayakumar, R. The structure of antimicrobial pexiganan peptide in solution probed by Fourier transform infrared absorption, vibrational circular dichroism, and electronic circular dichroism spectroscopy. *Biopolymers* **2005**, *80*, 636–642.

(65) Liu, Z.; Chen, K.; Ng, A.; Shi, Z.; Woody, R. W.; Kallenbach, N. R. Solvent dependence of PPII conformation in model Alanine peptides. *J. Am. Chem. Soc.* **2004**, *126*, 15141–15150.

(66) Matthews, J. M.; Ward, L. D.; Hammacher, A.; Norton, R. S.; Simpson, R. J. Roles of histidine 31 and tryptophan 34 in the structure, self-association, and folding of murine interleukin-6. *Biochemistry* **1997**, *36*, 6187–6196.

(67) White, S. H.; Wimley, W. C. Membrane protein folding and stability: Physical Principles. *Annu. Rev. Biophys. Biomol. Struct.* **1999**, *28*, 319–365.

(68) Bonomo, R. P.; Cucinotta, V.; Giuffrida, A.; Impellizzeri, G.; Magrì, A.; Pappalardo, G.; Rizzarelli, E.; Santoro, A. M.; Tabbì, G.; Vagliasindi, L. I. A re-investigation of copper coordination in the octa-repeats region of the prion protein. *Dalton Trans.* **2005**, 150–158.

JP1033036